Experimental evidence of shell effects in slow quasifission

A. Pal,[1,2,*] S. Santra,[1,2,†] P. C. Rout,[1,2] A. Kundu,[1,‡] D. Chattopadhyay,[1,§] Ramandeep Gandhi,[1,2] P. N. Patil,[3] R. Tripathi,[2,4] B. J. Roy,[1,2] Y. Sawant,[1] T. N. Nag,[2,4] Abhijit Baishya,[1,2] T. Santhosh,[1,2] P. K. Rath,[5] and N. Deshmukh[6]

[1]*Nuclear Physics Division, Bhabha Atomic Research Centre, Mumbai 400085, India*
[2]*Homi Bhabha National Institute, Anushaktinagar, Mumbai 400094, India*
[3]*Department of Physics, KLE Technological University, Hubballi 580031, India*
[4]*Radio Chemistry Division, Bhabha Atomic Research Centre, Mumbai 400085, India*
[5]*Centurion University of Technology and Management, Paralakhemundi, Odisha 576104, India*
[6]*School of Sciences, PP Savani University, Dhamdod, Kosamba, Surat 394 125, India*

(Received 2 February 2023; revised 6 June 2024; accepted 8 August 2024; published 3 September 2024)

Mass distributions of fission fragments arising from the slow quasifission (SQF) process, derived by comparing the measured data with theory for several reactions, show distinct features. Irrespective of fissioning systems, the peak corresponding to lighter fragments in the SQF mass distribution is found to be always at $A \approx 96$, whereas the peak position of the heavier fragments increases linearly with the mass of the dinuclear system. Further, the yield of quasifission events decreases with the increasing projectile energy. These observations within certain model dependence provide clear evidences of shell effect in slow quasifission, where the lighter fragments are possibly some closed-shell nuclei in the mass region $A \approx 96$ (possibly ^{96}Zr or ^{94}Sr). Further, the results from a model independent approach involving multi-Gaussian fit to the high energy data points reaffirm the above conclusion.

DOI: 10.1103/PhysRevC.110.034601

I. INTRODUCTION

While synthesizing superheavy elements (SHE) using fusion reactions [1–6], a preequilibrium fission reaction mechanism, generically named as quasifission (QF) [7–9], has been known since the mid-1970s as a cause for the suppression of SHE formation. Since then many aspects of QF have been explored experimentally by measuring fission fragment (FF) mass and angular distributions [10–28] and theoretically by developing many macroscopic and microscopic dynamical models [29–33]. From the above studies, one can broadly classify the QF process into two categories: fast and slow quasifission. The fast quasifission (FQF) which is generally observed in reactions with heavy targets and projectiles, having charge product (Z_pZ_t) more than 1500, is accompanied by very asymmetric mass distributions, fast time scales ($\approx 10^{-20}$ s), and mass-angle correlation [13–21]. In contrast, the slow quasifission (SQF) which is observed in reactions involving much lighter projectiles such as ^{9}Be, ^{11}B, ^{12}C, and ^{16}O, with actinide targets, is characterized mainly by a time scale intermediate to FQF and compound nuclear fission (CNF), nearly symmetric mass distributions, absence of mass-angle correlations, larger mass width from the most symmetric entrance channel populating the same compound nucleus, and sudden enhancement in the mass width at lower incident energies [22–28].

Recently the microscopic shell effect has been invoked to explain the mass distributions in the quasifission process [34–38]. Theoretically, based on a recent time dependent Hartree-Fock calculation on ^{50}Ca + ^{176}Yb reaction partners [37] forming the ^{226}Th composite system, it was found that the same deformed shell with $Z_H \approx 54$ as that of the S-II mode [39–43] in asymmetric fission of actinides is responsible for stopping mass equilibration in the fast quasifission process, without allowing the system to form a compound nucleus. In another calculation on the ^{48}Ca + ^{249}Bk system [44], the role of deformed shell closed nuclei with $N = 56$ on fast quasifission was reported. Experimentally also evidence for the role of proton shell closure ($Z = 82$) in fast quasifission reactions has been observed recently [38]. However, to date, there is no investigation on the role of shell effect in the SQF reaction mechanism. Actually, in a slow quasifission process, the nucleon exchange takes place from heavier (T) to lighter (P) colliding partners, in contrast to the compound nucleus formation process, as illustrated in Figs. 1(a) and 1(b). We can strongly anticipate that if one of the fragments becomes shell closed during the mass equilibration process in the SQF process, the dinuclear system breaks into two fragments resulting in a doubly peaked mass distribution, while mass distributions in the compound nuclear fission process are a superposition of several fission modes (superlong, S-I, S-II, etc.) depending on the excitation energy

*Contact author: asimpal@barc.gov.in
†Contact author: ssantra@barc.gov.in
‡Present address: Saha Institute of Nuclear Physics, 1/AFBidhannagar, Kolkata 700064, India.
§Present address: Department of Physics, The ICFAI University Tripura, West Tripura 799210, India.

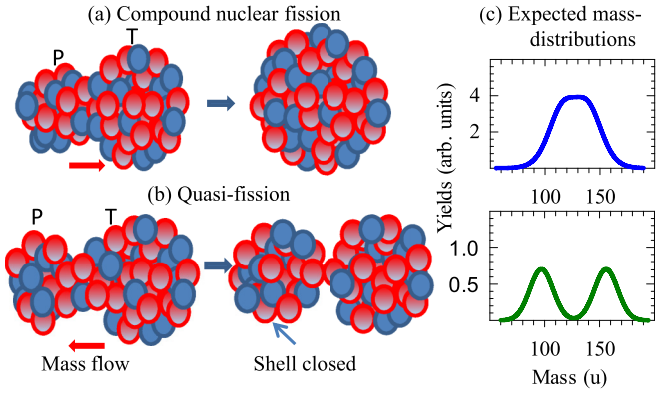

FIG. 1. Illustration of (a) compound nuclear fission process, (b) quasifission process, and (c) expected mass distributions in both the processes

and angular momenta populated in the system [Fig. 1(c)]. However, experimentally it is impossible to distinguish the fragments arising from CNF and SQF processes unless we take help from theoretical models incorporating CNF process.

In the present paper, FF mass distributions have been measured in the $^{19}F + ^{238}U$ reaction and compared with the theoretical model calculations. From the differences observed between the measured data and the calculation, the mass distributions and the probabilities corresponding to the QF process have been obtained at different projectile energies for the present system and the other systems for which FF mass distributions are available in literature. From the derived mass distributions of the QF process for different systems, we attempt to search for the quantum shell effect in the slow quasifission process, towards the development of complete understanding of quasifission mechanism and to improve the models in reaching reliable predictive capacities of SHE formation cross sections.

II. EXPERIMENT AND RESULTS

Fission fragments have been measured for the $^{19}F + ^{238}U$ reaction using pulsed beams (full width at half maximum $\approx$1 ns) of energies ranging from 99.7 to 142.1 MeV at the BARC-TIFR Pelletron-Linac facility, Mumbai. The details of the experimental setup and analysis procedure are the same as in Ref. [43]. The full momentum transfer events have been selected using a tight gate on the $v_{\parallel} - v_{cn}$ versus $v_{\parallel}$ plot as shown in Fig. 2(a) and analyzed for the present paper. The derived mass distributions are normalized to 200% as shown in Figs. 2(e)–2(h) by black circles. Data from our previous measurement on the same reaction at lower energies are shown in Figs. 2(b)–2(d) by green circles. The measured distributions were compared with the calculations (red solid lines in Fig. 2) using a semiempirical model code GEF [45,46] (a model well validated for light particle induced fission) based on compound nuclear fission and found to be wider, especially at lower beam energies. To rule out the fact that the broadening of the measured data is due to the limited mass resolution of the experimental setup, the calculated distributions have been broadened incorporating the mass resolution of the experimental setup, $\sigma \approx 6$ u, as shown by blue dashed lines in Fig. 2. But, they failed to explain the much wider measured data and hint at possibilities of having admixture of quasifission along with the compound nuclear fission. Now, the width of the FF mass distribution as a function of compound nuclear excitation energy has been compared with the GEF calculations as shown in Fig 2(i) where a large deviation is observed at lower excitation energies, indicating significant contributions of the quasifission at below barrier energies, and it decreases with the increase in beam energy.

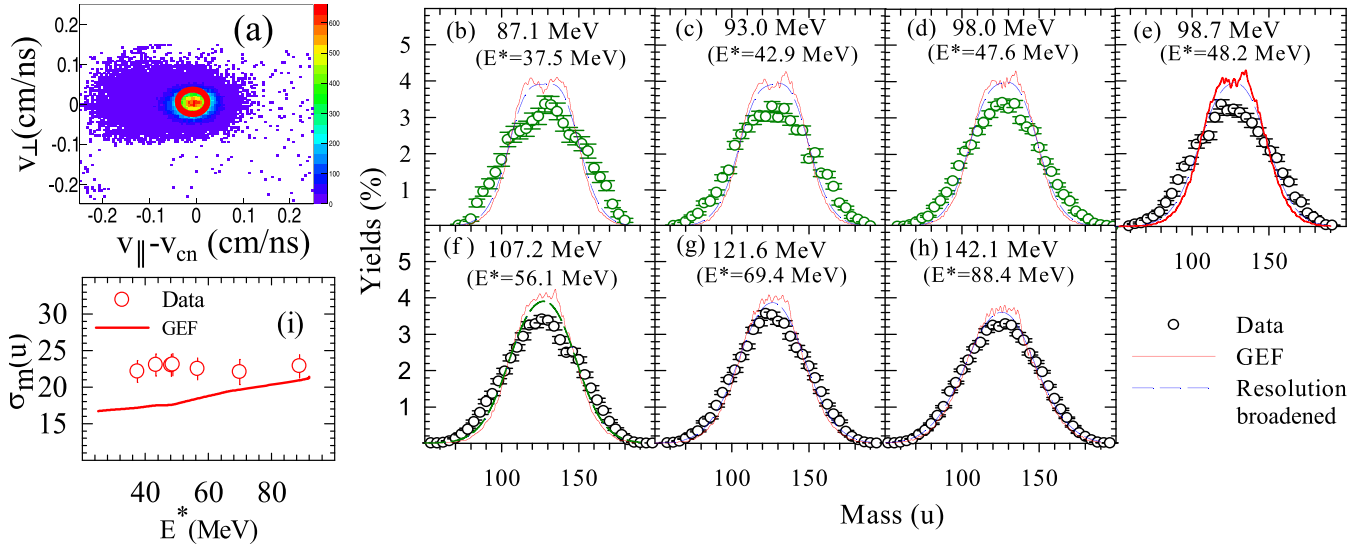

FIG. 2. (a) Typical "$v_{\parallel}$-v_{cn}" vs "$v_{\perp}$," obtained for $^{19}F + ^{238}U$ reaction at $E_{beam} = 142.1$ MeV. (b)–(d) Previously and (e)–(h) presently measured FF mass distributions, where data points are shown by symbols, the red solid lines represent the mass distribution obtained from the model GEF, and the blue dashed lines represent the distribution obtained after broadening the actual distribution by experimental mass resolution. (i) Width of the measured (circles) and calculated (solid line) mass distributions.

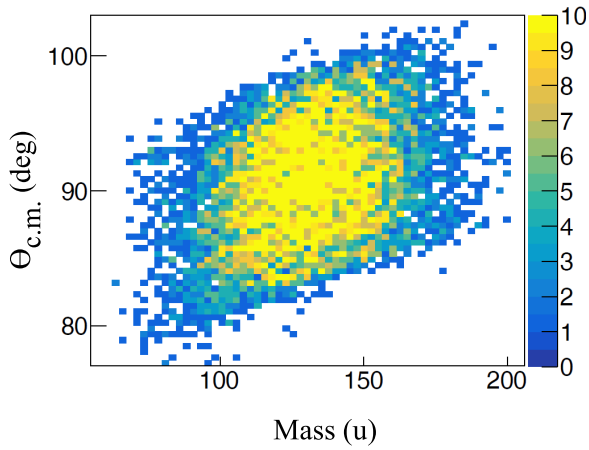

FIG. 3. Typical mass-angle correlation obtained for the present system at 98.7-MeV projectile energy.

Interestingly, neither a winglike structure in the asymmetric mass region of the experimental data (see Fig. 2) nor any mass-angle correlation (see Fig. 3) was observed for the present system. These observations are found to be consistent with several other systems available in the literature where the mass-angle correlations were measured over wide angular ranges [24]. This rules out the presence of fast quasifission but confirms the presence of slow quasifission. Though evidences for slow quasifission have already been observed by studying the FF angular anisotropies in reactions involving projectiles like ^{9}Be, ^{12}C, and ^{16}O [24], the evidence of slow quasifission has been obtained from the FF mass distribution in the present paper.

The two contributions, i.e., compound nuclear and slow quasifission processes, are then segregated from the measured mass distributions using a theoretical model that calculates the mass distributions following the compound nuclear fission process reliably. The quasifission is expected to produce mass asymmetric fragments [37], whereas the mass symmetric fragments are mostly originated from compound nuclear fission. So, theoretical mass distributions based on compound nuclear fission are normalized to the experimental mass yield at fragment mass $= 0.5 \times$ compound nuclear mass and then subtracted from the experimental data, resulting in the mass distributions due to QF process alone. For illustration, the measured data (filled rhombus), un-normalized theoretical distribution (dashed line), and normalized theoretical distribution (solid line) are shown in Fig. 4(a) for 98-MeV projectile energy. The QF mass distribution derived from the subtraction of data (filled diamonds) and normalized calculation (solid line) for the same 98-MeV data is shown by hollow diamonds in Fig. 4(b). It may be mentioned that a similar procedure was employed by Gupta *et al.* [47] showing that there is a presence of quasifission in the ^{37}Cl + ^{154}Sm reaction, but not in the ^{16}O + ^{175}Lu reaction forming the same compound nucleus.

Following the same procedure, mass distributions from the QF process for all the beam energies are obtained and shown in Figs. 4(b)–4(d). The QF mass distributions are then fitted using double Gaussian functions to extract the peak

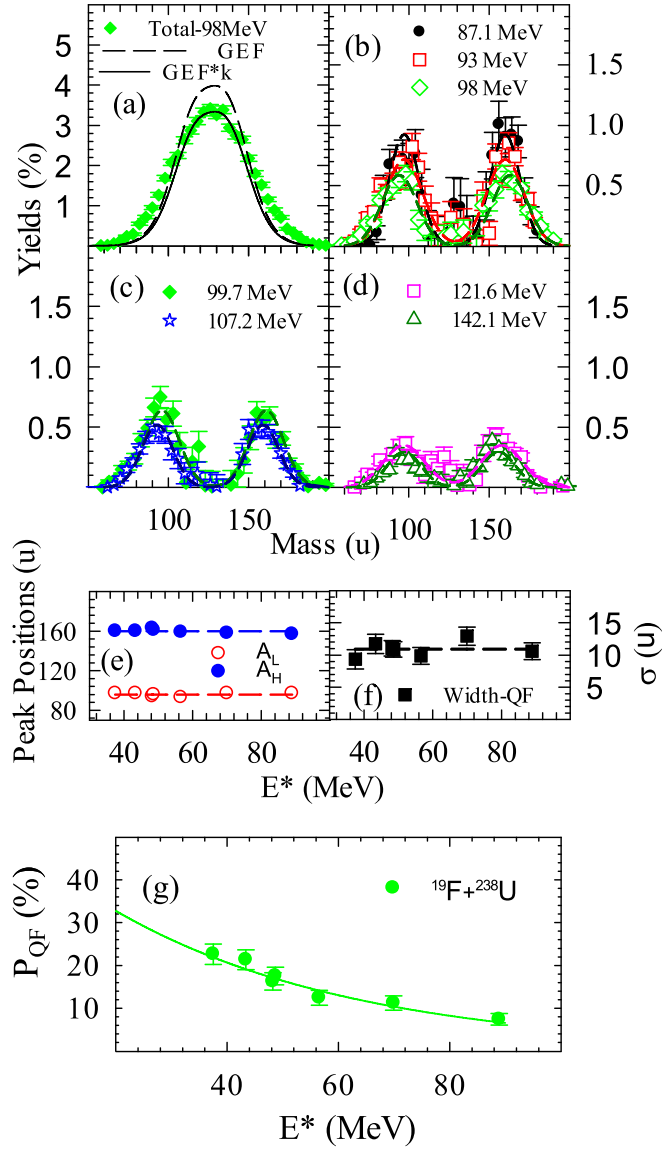

FIG. 4. (a) Comparison of measured, actual, and normalized calculated distributions. (b)–(d) Derived mass distributions corresponding to QF process at different projectile energies. (e), (f) Peak positions and width of the QF modes. (g) Quasifission probability for the present system.

positions, their widths, and fractional contribution of QF to total fission. Peak positions and widths of light and heavy fragments are shown in Figs. 4(e) and 4(f) respectively. It can be observed that for all the beam energies, the mean centroids of the two peaks are located at $A = 97 \pm 1$ and $A = 160 \pm 1$. It is also interesting to note that the peak heights and hence the contributions from the QF process gradually decrease with the increasing beam energies. Both these observations hint at possible shell effect in slow QF process. As already discussed earlier, in a nuclear collision event, when a dinucleus is formed after penetration of the Coulomb barrier, mass flow can take place from the projectile to the target and vice versa. The former lead to the formation of a compound nucleus followed by the splitting of the nucleus into two

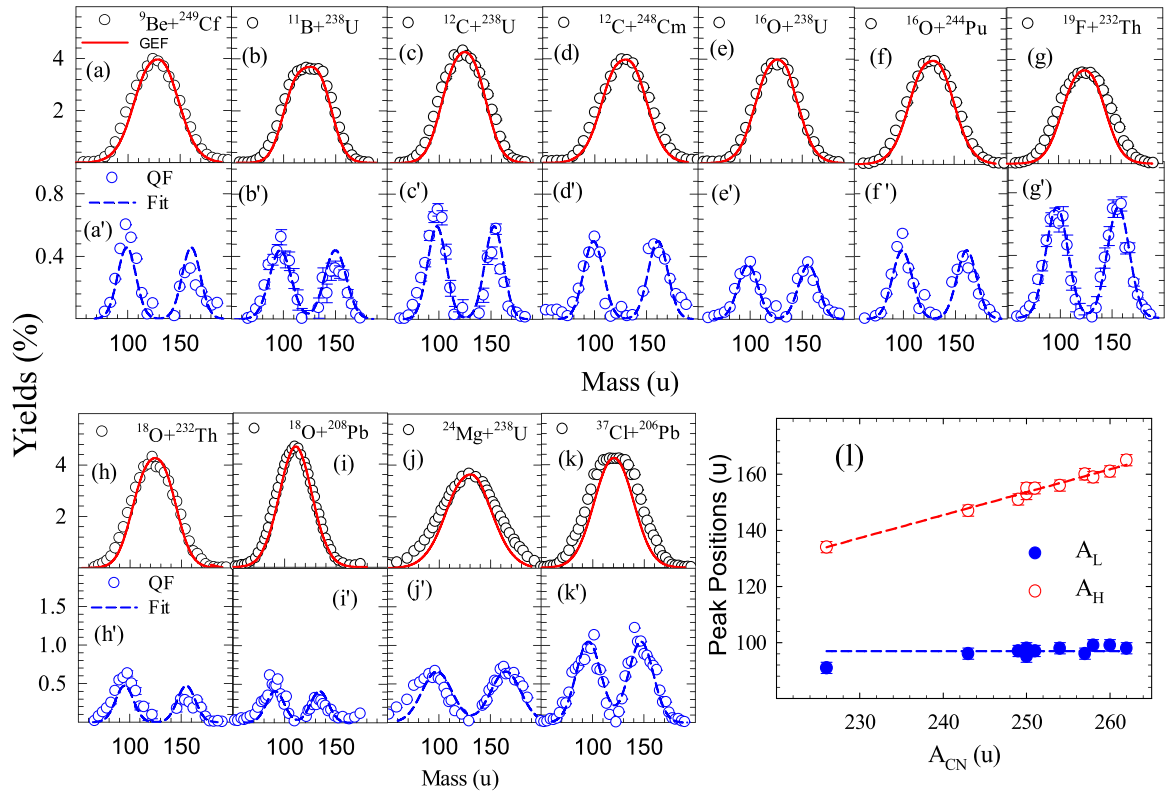

FIG. 5. (a)–(k) Comparison of measured data with normalized GEF calculations for reaction systems available in the literature. (a′) − (k′) Derived mass distributions for QF mode for respective systems. (l) Peak positions of light and heavy fragments of QF mass distributions.

fragments. Now if the initial mass asymmetry (α) is less than the Businaro-Gallone parameter (α_{BG}) [48], which is true for the present case as $\alpha = 0.85 < \alpha_{BG} = 0.93$, the mass flow from the target to the projectile is possible. In such cases, during the process of mass equilibration of the dinuclear system, if one of the nuclei achieves the shell closed configuration, the dinuclear system splits into two fragments without achieving the full mass-equilibration (compound nuclear formation) process. But, if the projectile energy is increased, the nucleons participating in the mass-equilibration process gain more excitation energies which will result in reduction of the above shell effect in the fragment and hence reduction in the QF probability.

The QF probability (the ratio of the QF yield to total fission yield) obtained as a function of compound nuclear excitation energy has been shown in Fig. 4(g) by green solid circles for the present system. It can be observed that the probability decreases with the increase in excitation energy. It is also interesting to note that the QF probability is significant even beyond the excitation energy of 80 MeV. It is worth mentioning here that the excitation energy in the dinuclear system is actually less than the compound nuclear excitation energy as the kinetic energy does not get fully transformed into excitation energy due to incomplete mass equilibration, thus resulting in pronounced shell effect in the slow quasifission process. It is really hard to calculate actual excitation energy in the dinuclear system undergoing slow quasifission process. The large deviations of angular anisotropy data as compared to the statistical model calculations at below barrier energies for several systems [49–52] suggest that the preequilibrium fission contribution is dominant at low energies. An attempt on the determination of slow quasifission probability has been made from the experimental angular anisotropy [14]. However, the mass distributions have been used to obtain the slow QF probability as an exponentially decaying function of compound nuclear excitation energy (E^*), i.e., $P_{QF}(E^*) = Ce^{-mE^*}$, where C and m are fitting parameters with values of 51.97 and 0.023 MeV^{-1} respectively for the present system. The fitted results have been shown by green line in Fig. 4(g).

Similar analysis has been performed for the mass distribution data of other reaction systems involving heavy projectiles and heavy targets available in the literature. The mass distributions corresponding to QF process have been obtained for different reaction systems at different excitation energies. The experimental FF mass distributions and the GEF calculations at excitation energies close to 50 MeV have been shown for the reaction systems ^{9}Be + ^{249}Cf [24], ^{11}B + ^{238}U [53], ^{12}C + ^{238}U [23], ^{12}C + ^{248}Cm [24], ^{16}O + ^{238}U [54], ^{16}O + ^{244}Pu [24], ^{18}O + ^{232}Th [23], ^{24}Mg + ^{238}U [14], and ^{37}Cl + ^{206}Pb [55] in Figs. 5(a)–5(k). The data shown in Fig. 5(i) for the ^{18}O + ^{208}Pb [18] system correspond to the compound nuclear excitation energy of 87 MeV. The corresponding QF modes for each system [Figs. 5(a′)–5(k′)] derived using the same method have been shown just below the respective mass distribution plots. It can be observed that

the QF mass distributions are clearly doubly peaked for all the systems.

The QF mass distributions for all the above systems have been fitted with double Gaussian functions and the peak positions of the light and heavy fragments are plotted as a function of compound nuclear mass A_{CN} in Fig. 5(l). It is interesting to note that the peak position corresponding to the light fragment is more or less constant around $A = 96$, whereas the mass of the heavy fragment increases with the mass of the fissioning nuclei. This observation is very analogous to the one for asymmetric fission in actinides where the mass of the heavy fragment does not change with the mass of the fissioning nuclei, but the light fragment does [56]. The fixed position of the peak of the heavier fragments in the asymmetric fission of actinides indicates the role of deformed shell closed nuclei with $Z_H \approx 52$–56 [39,57]. Similarly, the fixed peak position of the lighter fragments in the asymmetric fission of sublead nuclei suggests the role of shell closed nuclei with $Z_L \approx 34$–38 [58]. Using the same analogy, the present observation of the fixed position of the lighter mass peak in the SQF mass distribution can be treated as a clear evidence of the shell effect in the slow-quasifission process.

Before we predict the species of the lighter fragment, it may be appropriate to recollect about the types of closed-shell nuclei, either spherical or deformed, which have been observed to play the key role in the processes of nuclear fission and quasifission. In the actinide mass region, (1) the standard-I mode of fission is observed due to the role of the doubly magic spherical shell gap at $Z = 50$ and $N = 82$ [39,46], (2) the standard-II mode of fission is observed due to the role of the octupole deformed shell gap at $Z = 52$–56 [40], and (3) the standard-III mode emerges due to the role of the nearly spherical shell gap at $N = 52$ [59]. However, in the fission of sublead nuclei, the deformed shell closure at $Z \approx 34$–38 and 46 is found to be responsible for the distinct type of asymmetric fission mode [58,60]. On the other hand, in the case of quasifission process, a proton shell closure at $Z = 82$ (the corresponding nucleus is not exactly known) [38], the octupole deformed shell closure at $Z \approx 52$–56 (the corresponding nucleus is around ^{139}Cs) [37], and the octupole deformed shell closure at $N = 56$ (the corresponding nucleus is ^{94}Sr) [44] are shown to be playing important roles in $^{48}\mathrm{Ti} + ^{238}\mathrm{U}$, $^{50}\mathrm{Ca} + ^{176}\mathrm{Yb}$, and $^{48}\mathrm{Ca} + ^{249}\mathrm{Bk}$ reaction systems, respectively. Among all the closed-shell nuclei discussed above, only ^{94}Sr is the one whose mass number matches closely with the observed mass number that seems to govern the slow quasifission in the present paper. However, in the same mass region $A \approx 96$, there is another nucleus ^{96}Zr which qualifies to be a spherically shell closed nucleus as described in both the theoretical [61] and experimental work [62,63], which may also play an important role in the slow quasifission process.

Now, the QF probabilities derived from the FF mass distributions for other available reaction systems are also shown in Fig. 6(a) by different symbols and colors, all of which show a trend similar to the present system. The QF probabilities are then fitted using the same expression for $P_{QF}(E^*)$ by keeping the same value of parameter m as earlier but different values of C for different systems and the results are shown by the solid

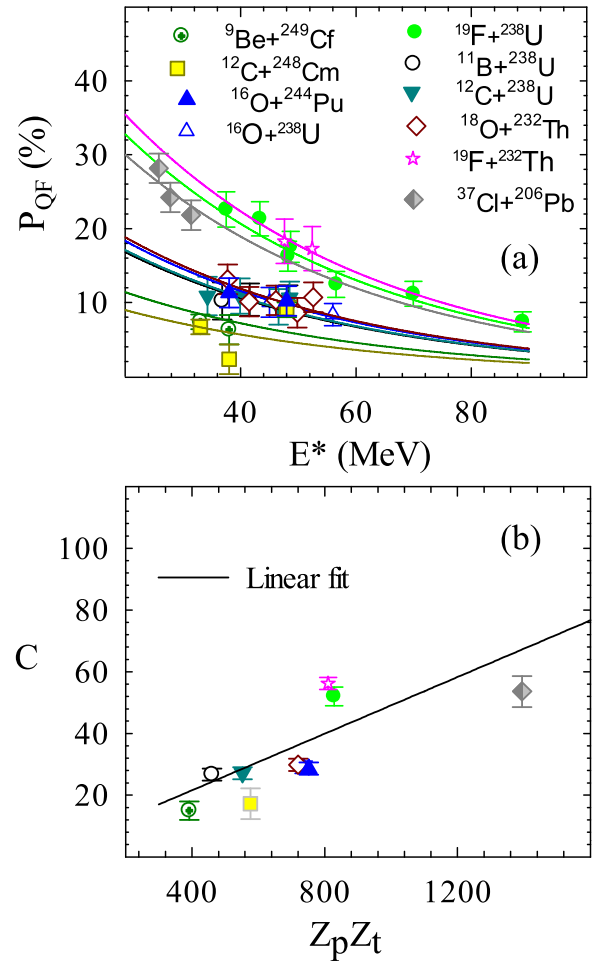

FIG. 6. (a) Quasifission probability obtained as a function of excitation energy for different reaction systems where the fits for each system are shown by solid lines with colors matching with respective symbols. (b) Variation of the fitting parameter C with the product of the charges of the projectile (Z_p) and the target (Z_t) and a linear fit (solid line) to the data points.

lines with the same color as that of the symbols in Fig. 6(a). From Fig. 6(b), it was interesting to observe that the value of C increases almost linearly with the product of target and projectile charges Z_pZ_t, i.e., $C = a + bZ_pZ_t$ with a (≈ 3) and b (≈ 0.05) as constants. Thus, for any reaction system with given Z_pZ_t value, one can estimate the probability of slow QF which is one of the responsible processes for inhibiting the SHE formation.

So far, the analysis and observations have been made based upon the predictions of a compound-nuclear fission model. In order to support the above observations another approach involving single and multi-Gaussian fits has been adopted following the work by Swinton-Bland *et al.* [64]. Here, we have considered the mass distributions measured at the two highest energies as the contributions from any asymmetric compound-nuclear fission mode are expected to be negligibly small at such high excitation energies. From Figs. 7(a) and 7(b) one can observe that, for both the energies, the single Gaussian functions fail to fit the data well, which is also very

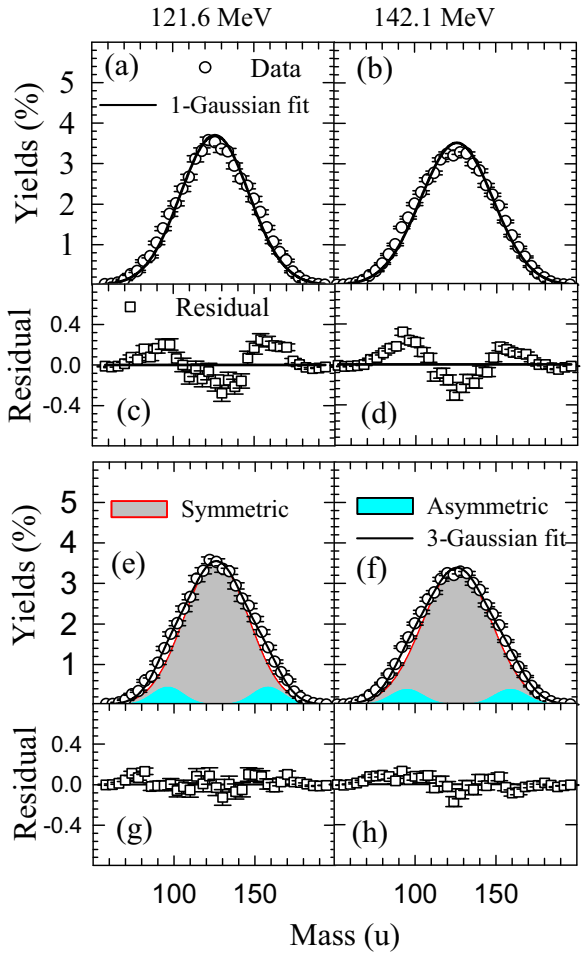

FIG. 7. (a), (b) Fitting of the mass distributions using the single Gaussian function and (c), (d) the residual values at 121.6 MeV and 142.1 MeV, respectively. (e), (f) Fitting of the mass distributions using the three-Gaussian function and (g), (h) the residual values for the same two energies.

clearly evident from the respective residual values shown in Figs. 7(c) and 7(d). The observed structures in the residual values of the single-Gaussian fits suggest the necessity of multi-Gaussian fit. Therefore, the same set of data has been fitted with three-Gaussian functions (out of which one represents the symmetric mode and the remaining two represent the asymmetric mode) and shown in Figs. 7(e) and 7(f). It is interesting to observe that the three-Gaussian fit explains the data very well as evident from the residual plots shown in Figs. 7(g) and 7(h). As already pointed out, here the asymmetric mode must correspond to the slow quasifission mode as any asymmetric compound nuclear fission mode is expected to wash out at such high excitation energies. It is also interesting to note that the peak positions of the asymmetric mode are found to be at $A_L \approx 96$ and $A_H \approx 161$ for both the energies, which is in excellent agreement with the observations made earlier in this paper for slow-quasifission modes. The yields of the asymmetric mode are also comparable with the ones obtained earlier in the present paper. Thus, the above model-independent approach reaffirms the conclusions drawn on the slow quasifission mode using the compound nuclear fission model GEF.

III. SUMMARY AND CONCLUSION

In summary, the differences observed between the measured fission fragment mass distributions and the calculations incorporating the compound nuclear fission process for several reaction systems suggest that the measured data contain contributions not only from the CN fission but also from the slow QF processes. It is interesting to observe that, for a particular reaction system, the peak positions of the doubly peaked QF mass distributions do not change but the peak heights decrease with the increase in beam energy. Most importantly, it was observed that the peak position for the lighter fragment remains unchanged around $A = 96$ whereas that of the heavier fragment increases with the mass of the dinuclear system.

All of the above observations can be treated as clear evidences of quantum shell effect in slow quasifission process. Therefore the present paper reveals the role of some shell closed nuclei in the mass region $A \approx 96$, governing the mechanism of the slow quasifission reaction. Our result is quite close to the theoretical observation by Godbey *et al.* [44], where the strong influence of the octupole deformed shell gap at $N = 56$ (corresponding nucleus ^{94}Sr) is observed to govern the quasifission process. It is known from the literature that ^{96}Zr is a spherical closed-shell nucleus which can also be a possible candidate responsible for the observed shell effect.

Further, an empirical expression has been obtained from the present systematics that can predict the contribution of slow QF process for a given charge product of two colliding partners. Thus the present results will not only enhance the capabilities of the nuclear models for reliable predictions of SHE formation cross sections but also trigger theoretical and experimental investigations in the field of nuclear reactions, structure, and superheavy element synthesis.

It may be mentioned here that the net contributions in the measured mass distributions from the symmetric and asymmetric modes of the fusion-fission events are estimated with the help of the GEF model calculations and the conclusions drawn in the present paper are made under the assumption that the symmetric components in the mass distributions are entirely due to the fusion-fission events, which may not be entirely true as it may contain some quasifission component as well. However, a model-independent approach involving single- and multi-Gaussian fits to the high-energy data points leads to the same conclusion on the slow quasifission modes as obtained using the above model.

ACKNOWLEDGMENTS

Fruitful discussions with K.-H. Schmidt are thankfully acknowledged. We thank the Pelletron crew for smooth running of the accelerator during the experiment.

[1] Y. T. Oganessian *et al.*, Phys. Rev. C **70**, 064609 (2004).
[2] Y. T. Oganessian *et al.*, Phys. Rev. C **74**, 044602 (2006).
[3] Y. T. Oganessian, J. Phys. G **34**, R165 (2007).
[4] Y. T. Oganessian *et al.*, Phys. Rev. Lett. **104**, 142502 (2010).
[5] Y. Oganessian and V. Utyonkov, Rep. Prog. Phys. **78**, 036301 (2015).
[6] S. N. Dmitriev *et al.*, Mendeleev Commun. **15**, 1 (2005).
[7] J. Peter, C. Ngo, and B. Tamain, Nucl. Phys. A **250**, 351 (1975).
[8] R. Bock *et al.*, Nucl. Phys. A **388**, 334 (1982).
[9] J. Toke *et al.*, Nucl. Phys. A **440**, 327 (1985).
[10] V. S. Ramamurthy and S. S. Kapoor, Phys. Rev. Lett. **54**, 178 (1985).
[11] D. J. Hinde, M. Dasgupta, J. R. Leigh, J. P. Lestone, J. C. Mein, C. R. Morton, J. O. Newton, and H. Timmers, Phys. Rev. Lett. **74**, 1295 (1995).
[12] V. S. Ramamurthy *et al.*, Phys. Rev. Lett. **65**, 25 (1990).
[13] D. J. Hinde, R. duRietz, M. Dasgupta, R. G. Thomas, and L. R. Gasques, Phys. Rev. Lett. **101**, 092701 (2008).
[14] D. J. Hinde *et al.*, Phys. Rev. C **97**, 024616 (2018).
[15] R. Rafiei, R. G. Thomas, D. J. Hinde, M. Dasgupta, C. R. Morton, L. R. Gasques, M. L. Brown, and M. D. Rodriguez, Phys. Rev. C **77**, 024606 (2008).
[16] E. Prasad, A. Wakhle, D. J. Hinde, E. Williams, M. Dasgupta, M. Evers, D. H. Luong, G. Mohanto, C. Simenel, and K. Vo-Phuoc, Phys. Rev. C **93**, 024607 (2016).
[17] E. M. Kozulin *et al.*, Phys. Rev. C **94**, 054613 (2016).
[18] M. G. Itkis, E. Vardaci, I. M. Itkis, G. N. Knyazheva, and E. M. Kozulin, Nucl. Phys. A **944**, 204 (2015).
[19] M. G. Itkis *et al.*, Nucl. Phys. A **787**, 150 (2007).
[20] A. Sen, T. K. Ghosh, E. M. Kozulin, I. M. Itkis, G. N. Knyazheva, K. V. Novikov, S. Bhattacharya, K. Banerjee, and C. Bhattacharya, Phys. Rev. C **105**, 014627 (2022).
[21] M. Morjean *et al.*, Phys. Rev. Lett. **101**, 072701 (2008).
[22] R. G. Thomas, D. J. Hinde, D. Duniec, F. Zenke, M. Dasgupta, M. L. Brown, M. Evers, L. R. Gasques, M. D. Rodriguez, and A. Diaz-Torres, Phys. Rev. C **77**, 034610 (2008).
[23] C. Yadav *et al.*, Phys. Rev. C **86**, 034606 (2012).
[24] T. Banerjee *et al.*, Phys. Rev. C **102**, 024603 (2020).
[25] K. Banerjee *et al.*, Phys. Rev. C **83**, 024605 (2011).
[26] T. K. Ghosh, S. Pal, T. Sinha, N. Majumdar, S. Chattopadhyay, P. Bhattacharya, A. Saxena, P. K. Sahu, K. S. Golda, and S. K. Datta, Phys. Rev. C **69**, 031603(R) (2004).
[27] T. K. Ghosh *et al.*, Phys. Rev. C **79**, 054607 (2009).
[28] T. K. Ghosh, S. Pal, T. Sinha, S. Chattopadhyay, P. Bhattacharya, D. C. Biswas, and K. S. Golda, Phys. Rev. C **70**, 011604(R) (2004).
[29] A. Diaz-Torres, G. G. Adamian, N. V. Antonenko, and W. Scheid, Phys. Rev. C **64**, 024604 (2001).
[30] Y. Aritomo, K. Hagino, K. Nishio, and S. Chiba, Phys. Rev. C **85**, 044614 (2012).
[31] C. Simenel, Eur. Phys. J. A **48**, 152 (2012).
[32] C. Simenel, D. Hinde, R. du Rietz, M. Dasgupta, M. Evers, C. Lin, D. Luong, and A. Wakhle, Phys. Lett. B **710**, 607 (2012).
[33] K. Sekizawa and K. Yabana, Phys. Rev. C **93**, 054616 (2016).
[34] M. G. Itkis *et al.*, Nucl. Phys. A **734**, 136 (2004).
[35] A. Wakhle, C. Simenel, D. J. Hinde, M. Dasgupta, M. Evers, D. H. Luong, R. duRietz, and E. Williams, Phys. Rev. Lett. **113**, 182502 (2014).
[36] V. E. Oberacker, A. S. Umar, and C. Simenel, Phys. Rev. C **90**, 054605 (2014).
[37] C. Simenel, P. McGlynn, A. Umar, and K. Godbey, Phys. Lett. B **822**, 136648 (2021).
[38] M. Morjean *et al.*, Phys. Rev. Lett. **119**, 222502 (2017).
[39] C. Bockstiegel, S. Steinhauser, K. H. Schmidt, H.-G. Clerc, A. Grewe, A. Heinz, M. de Jong, A. R. Junghans, J. Muller, and B. Voss, Nucl. Phys. A **802**, 12 (2008).
[40] G. Scamps and C. Simenel, Nature (London) **564**, 382 (2018).
[41] S. Santra *et al.*, Phys. Rev. C **90**, 064620 (2014).
[42] A. Pal *et al.*, Phys. Rev. C **98**, 031601(R) (2018).
[43] A. Pal, S. Santra, P. C. Rout, R. Gandhi, A. Baishya, T. Santhosh, R. Tripathi, and T. N. Nag, Phys. Rev. C **104**, L031602 (2021).
[44] K. Godbey, A. S. Umar, and C. Simenel, Phys. Rev. C **100**, 024610 (2019).
[45] B. Jurado and K. H. Schmidt, Computer code GEF, version 1.2 (2020), http://www.khs-erzhausen.de/GEF-2020-1-2.html.
[46] K.-H. Schmidt, B. Jurado, C. Amouroux, and C. Schmitt, Nucl. Data Sheets **131**, 107 (2016).
[47] S. Gupta *et al.*, Phys. Lett. B **803**, 135297 (2020).
[48] U. L. Businaro and S. Gallone, Nuovo Cim. **5**, 315 (1957).
[49] S. Kailas, Phys. Rep. **284**, 381 (1997).
[50] R. G. Thomas, R. K. Choudhury, A. K. Mohanty, A. Saxena, and S. S. Kapoor, Phys. Rev. C **67**, 041601(R) (2003).
[51] A. Pal *et al.*, Phys. Rev. C **96**, 024603 (2017).
[52] S. Appannababu *et al.*, Phys. Rev. C **83**, 067601 (2011).
[53] S.Santra *et al.*, Phys. Rev. C **107**, L061601 (2023).
[54] T. Banerjee, E. M. Kozulin, N. T. Burtebayev, K. B. Gikal, G. N. Knyazheva, I. M. Itkis, K. V. Novikov, T. N. Kvochkina, Y. S. Mukhamejanov, and A. N. Pan, Phys. Rev. C **105**, 044614 (2022).
[55] G. Mohanto *et al.*, Phys. Rev. C **102**, 044610 (2020).
[56] K. F. Flynn, E. P. Horwitz, C. A. A. Bloomquist, R. F. Barnes, R. K. Sjoblom, P. R. Fields, and L. E. Glendenin, Phys. Rev. C **5**, 1725 (1972).
[57] K.-H. Schmidt *et al.*, Nucl. Phys. A **665**, 221 (2000).
[58] K. Mahata, C. Schmitt, S. Gupta, A. Shrivastava, G. Scamps, and K.-H. Schmidt, Phys. Lett. B **825**, 136859 (2022).
[59] S. Mulgin, V. Okolovich, and S. Zhdanov, Phys. Lett. B **462**, 29 (1999).
[60] R. Kumar *et al.*, Phys. Rev. C **107**, 034614 (2023).
[61] I. Boboshin, V. Varlamov, B. Ishkhanov, and E. A. Romanovsky, Phys. Atom. Nuclei **70**, 1363 (2007).
[62] L. Gan *et al.*, Phys. Rev. C **97**, 064614 (2018).
[63] D. A. Sazonov, E. A. Kolganova, T. M. Shneidman, R. V. Jolos, N. Pietralla, and W. Witt, Phys. Rev. C **99**, 031304(R) (2019).
[64] B. M. A. Swinton-Bland *et al.*, Phys. Lett. B **837**, 137655 (2023).